Dynamic Moduli of Elastomer Nano-Composites via Analytical and Molecular Modelling

Reinhard Hentschke

School of Mathematics and Natural Sciences, University of Wuppertal, Wuppertal, D-42097, Germany

ABSTRACT

I focus on the dynamic moduli of filled rubber and a novel strategy for their computation via molecular modelling. This work explores a theoretical methodology to predict tire performance parameter changes, e.g. changes in rolling resistance, in relation to alterations in a rubber material's chemical composition. The bridging of scales from times and sizes of the molecular domain to those of macroscopic samples is achieved by interlacing an analytical model with simulations on different level of coarse-graining. The model is for $\tan\delta$, the loss modulus divided by the storage modulus of the material, which is a laboratory indicator for rubber performance parameters in the tire industry. It is shown how $\tan\delta$ can be understood in terms of temperature or in terms of strain amplitude, including its dependence on filler particle size, filler loading or filler type. All parameters in the model possess clear physical meaning. The particular appeal of the final expression for $\tan\delta$ is its ability to relate chemical detail, which enters the model via independent molecular modelling calculations, to the aforementioned macroscopic tire performance parameters.

1 Introduction

'Chemistry by computer' has been part of the methodological tool chest of material developers in academia and industry for two or three decades (e.g.[1]). Nevertheless, it remains difficult to forsee the properties of materials on the macroscopic spatial or temporal scales in relation to their chemical composition or changes thereof. This 'scale-bridging problem' is often attacked by coarse-graining schemes. Another approach employs analytical models, containing parameters or functions thereof, which in turn can be modelled in the molecular domain. Here we summarize and extend work based on the latter approach to the prediction of the dynamic moduli in highly filled elastomers[2–4]. The specific quantity of interest is $\tan\delta$, the ratio of the loss modulus μ' to the storage modulus μ'', of rubbers. $\tan\delta = \mu''/\mu'$ is a useful laboratory indicator for tire performance parameters, because of its correlation to rolling resistance or grip under various road conditions (e.g.[5]). Thus, we shall discuss a model for $\tan\delta$, identify the parts of the model accessible to molecular modelling techniques and present a number of example results illustrating the general usefulness of this methodology. The model developed here allows to understand $\tan\delta$, either in terms of temperature or in terms of strain amplitude, and its dependence on filler particle size, filler loading or filler type. All parameters in the model possess clear physical meaning. The particular appeal of the final expression for $\tan\delta$ is its ability to relate chemical detail, which enters the model via independent molecular modelling calculations, to the aforementioned macroscopic tire performance parameters.

2 The Model

Figure 1 is a cartoon of the filler network traversing the rubber material. The filler network consists of the actual filler aggregates embedded in a 'polymer coat' of a certain thickness. In addition we concentrate on filler volume fractions $\phi > \phi_c$, where ϕ_c is the filler volume fraction at the percolation threshold. To a first approximation the material's storage modulus should be given by the sum of the two terms mathematically representing the bulk polymer and filler network in Fig. 1, i.e.

$$\mu' \approx \mu'_{\text{bulk poly}} + \left(\frac{\phi}{\phi_c}\right)^Y \frac{\gamma}{R} x_i x_{i,A}(T) h(u) \ . \tag{1}$$

Note that 'bulk polymer' in the present case may include a weak ϕ-dependence due to hydrodynamic reinforcement, for instance by including a factor $(1 + 5\phi/2)$[6].

Here we will be focussing on the filler network's contribution to the overall storage modulus, which is described by the second term. The factor ϕ^Y, where Y is a positive number, is well known and describes the structural filler reinforcement based on the notion of a self-similar or fractal filler distribution in the polymer matrix[6]. Based on this Y is found to be around 3.5, but may
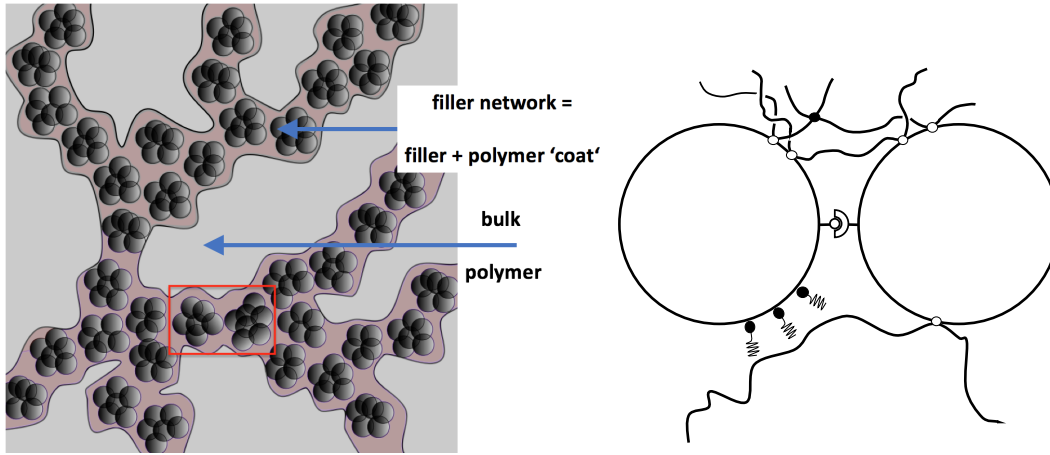
Figure 1. Left: Cartoon of a filled elastomer. The grey area is bulk polymer. The filler network is understood to consist of the actual filler aggregates embedded in a 'polymer coat' (reddish hue). Right: Different types of bonds connecting two aggregates depicted as large circles instead of lumps of smaller primary filler particles as in the left panel (top: Single polymer segment or cross-linked polymer segments bridging the gap between the particles (open circles: physical bonds; closed circle: chemical bond); center: The symbol in the center represents a strong direct bond (e.g. a hydrogen bridge in the case of silica); bottom: Silanes on the left aggregate prevent the physisorption of the polymer segment.)

vary considerably in the experiments[7]. The remaining factor $R^{-1}x_i x_{i,A}(T)h(u)$ is discussed in detail in Ref.[4]. Here R is the aggregate size (or radius), which is found to be roughly proportional to the size of the primary particles[8]. The quantity x_i is the number fraction of bonds of type i between neighboring aggregates in a (load bearing) network strand. It is multiplied by $x_{i,A}(T)$, which is the fraction of i-bonds in the closed state at temperature T. Notice that the summation convention applies to $x_i x_{i,A}(T)$.

A bond can be a hydrogen bond between silanol groups on adjacent silica particles when the filler is silica. A bond can also be formed by a polymer segment physisorbed on a particle surface. If the polymer itself, or as part of a network strand, bridges the gap to an adjacent filler particle then this connection can serve as a bond as well. Similar bonds can be formed involving silanols. In general, a 'bond' can be every conceivable atomic or molecular bond, which can break reversibly (in a mechanical sense) under the influence of strain (cf. right panel in Fig. 1). Note that every bond type has its characteristic energy $E_{a,i}$, i.e. $x_{i,A} = x_{i,A}(T; E_{a,i})$. Notice also that $x_{i,A}(T; E_{a,i})$, which is calculated explicitly in Ref.[2], is monotonously decreasing function of temperature, whose rate of decrease depends on $E_{a,i}$. Typical values for $E_{a,i}$ vary between about $E_a = -10$ kJ/mol, for dispersion attraction between short polymer segments and particle surfaces, and $E_a = -25$ kJ/mol, for hydrogen bonding.

The function $h(u) = (1 - (D/d)u)^{-y}$, where u is the macroscopic strain amplitude, is the load-baring network strands distribution derived in Ref.[2], again based on the assumption of self-similarity. The ratio D/d is the (mean) aggregate diameter ($D = 2R$) divided by the (mean) inter-aggregate separation along a load-bearing network strand and y is a positive exponent. Plotting $h(u)$ versus $\log u$ yields the typical decrease $\Delta \mu'$ of the storage modulus depicted in the left panel of Fig. 2 - the Payne effect. The temperature dependence of $\Delta \mu'$ is given by $x_{i,A}(T)$.

We can understand the the meaning of the quantity γ more easily if we insert typical numbers into Eq. (1). For instance we may assume $\phi \approx 2\phi_c$ (e.g. for N220 the percolation threshold is around 30 phr[9]) or $(\phi/\phi_c)^{3.5} \approx 10$. In this case we expect $\mu' - \mu'_{\text{bulk poly}} \sim 10^7$ Pa at $u = 0$ (which means $h(u = 0) = 1$). We also expect that $x_i x_{i,A}$ between 0.1 to 1. In addition we have $R \sim 10^{-8}$ m. Thus we find that γ is between 10 to 100 in units of mJ/m^2. This is a very plausible range for interfacial free energies in the systems of interest[10]. It is particularly pleasing that this range arises naturally on the basis of other typical numbers within this context. Notice that interfacial free energies in general are functions of temperature. Our γ refers to the hypothetical limit when $x_{i,A} = 1 \ \forall i$, the entire temperature dependence is absorbed in the quantities $x_{i,A}$.

We now turn to the loss modulus μ''. In the linear theory the dissipated energy density is $w \propto \mu'' u^2$, where the proportionality constant is of no immediate importance. Even if the system becomes non-linear, as is the case for filled elastomers, we may continue to use this as a definition. In fact this is how most rheological data are analysed - even if the material is non-linear.

As before in the case of μ' we approximate μ'' as a sum of a contribution from the bulk polymer plus a contribution from the network, i.e.
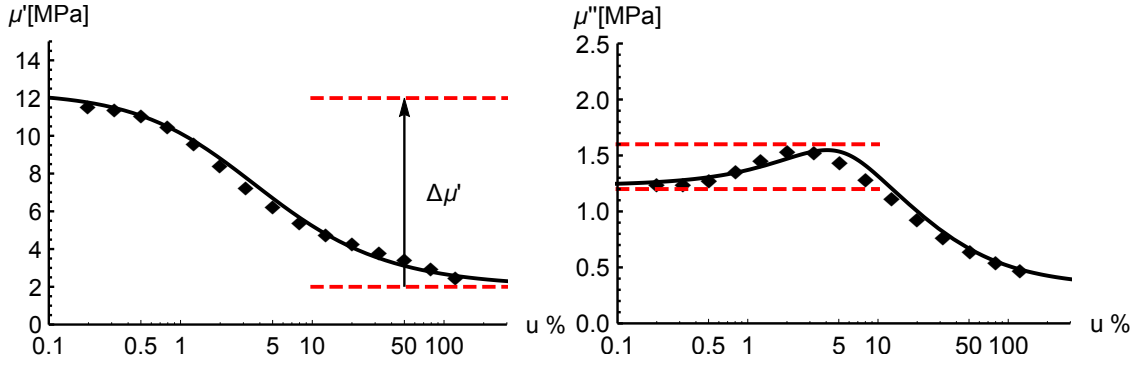
Figure 2. Illustration of the characteristic shape of the storage and loss moduli vs. strain amplitude. Left panel - dashed lines: Payne effect. Right panel - dashed lines: modulus depression at small strain amplitude u caused by strain inhomogeneity.

$$\mu'' \approx \mu''_{\text{bulk poly}} + \left(\frac{\phi}{\phi_c}\right)^Y \frac{W_{\text{loss}}(T)}{R} \frac{1}{u^2} \int_0^u du' \int_0^\infty d\delta u f(\delta u, u') \left(1 - h(u')\right) . \tag{2}$$

Again we concentrate on the second term in Eq. (2), i.e. the filler network's contribution to μ''. The factor u^{-2} indicates the application of a linear analysis. The remainder basically accounts for w contributed by the network. The central element dissipating energy is the contact between neighboring aggregates in a network strand (cf. the red box in the network cartoon depicted in Fig. 1). Externally applied strain may cause a contact to open. If the strain is relaxed the contact may close again. Closing means that bonds in the the above sense will close, i.e. we consider reversible bonds only at this point. Notice that 'reversible' here does not mean thermodynamic reversibility. It merely means that the bonds can open and close, but that this process is accompanied by energy dissipation in the contact. But how many contacts do contribute to $\mu''(u)$ in a strain sweep from 0 to u? Naively we assume that this number is proportional to $\int_0^u du'(1 - h(u'))$, where $h(u')$ is the distribution of load-bearing network paths. The normalization is such that $h(u' = 0) = 1$, which means that the number of contributing contacts vanishes when the strain amplitude is zero. It is important to note that this does not imply that the attendant loss modulus vanishes. In order to understand this we expand $1 - h(u')$ for small u', which yields $1 - h(u') \propto u'$. Therefore, this time for small u, we find $\int_0^u du'(1 - h(u')) \propto u^2$. Remembering the factor u^{-2} we find that $u^{-2} \int_0^u du'(1 - h(u'))$ approaches a constant in the limit $u \to 0$. This is in line with typical measurements as depicted in the right panel of Fig. 2. But what is the reason for the double integration in Eq. (2)? Notice that $h(u')$ and therefore $\int_0^u du'(1 - h(u'))$ decreases monotonously with increasing u' and u, respectively. This means that the characteristic maximum of $\mu''(u)$ cannot be described by $u^{-2} \int_0^u du'(1 - h(u'))$! This inconsistency with experimental evidence may be overcome by including the spatial non-uniformity of the strain amplitude throughout the material. In the following we make the simple assumptions that u' is an average and that the deviations from this average in different regions of the material can be described by a Gaussian distribution

$$f(\delta u, u') = \frac{1}{\sqrt{2\pi s^2}} \int_0^\infty d\delta u \exp[-(\delta u - u')^2/(2s^2)] . \tag{3}$$

Here the normalization is such that $\int_0^\infty d\delta u f(\delta u, u') \to 1$ if $u' \gg s$. The distribution is shown in Fig. 3 for three different values of u'/s. When $u' \gg s$ the integration over $d\delta u$ will always yield a number close to unity and there is no discernible effect on the amplitude dependence of $\mu''(u)$. If however u' becomes comparable or smaller than the width of the distribution, then the integration over $d\delta u$ yields smaller values between 1 and 0.5. This in turn will decrease $\mu''(u)$ if u is comparable to s as well (otherwise, i.e. $u \gg s$, the effect again will be negligible). Thus, the 'depression' of $\mu''(u)$ observed at small strain amplitudes is a consequence of the strain inhomogeneity within the material. The position of the maximum of $\mu''(u)$ is correlated with the width s of the distribution. We must note, however, that the Gaussian shape of the distribution merely is a simple assumption, i.e. shapes deviating from a Gaussian are possible and even likely. Nevertheless, the effect, i.e. the low-amplitude cut-off of the distribution, will persist! In Ref.[2] the interested reader can find approximations to the somewhat unwieldy double integral. The factor $(\phi/\phi_c)^Y R^{-1}$ arises due to the fractal nature of the filler distribution assumed here. It is the same for both the storage and the loss modulus contributions of the filler network. Finally there is the loss contribution of a contact per unit area, $W_{\text{loss}}(T)$. In Refs.[3] $W_{\text{loss}}(T)$ is studied applying molecular dynamics simulations to contacts between silica particles. The particles usually posses diameters between 4 to 6 nm, which still is smaller than the primary particle and of course the aggregate size
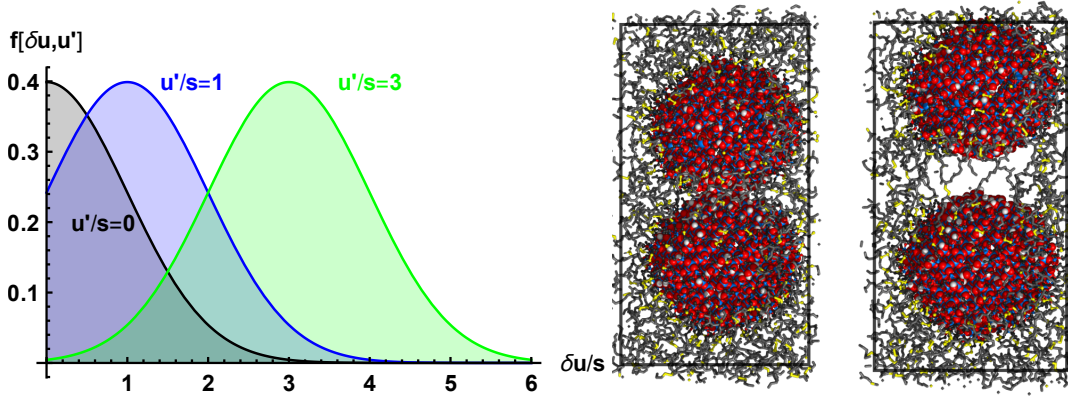
Figure 3. Left: Distribution function $f(\delta u, u')$. Right: A contact between filler particles (cf. the red box in left panel of Fig. 1), closed and open, simulated via molecular dynamics at atomic detail. Here the silanized silica particles are embedded in sulfur cross-linked polyisoprene.

in experimental systems. Nevertheless, we were able to identify two contributions to $W_{loss}(T)$. One is the viscous loss in the 'polymer coat' surrounding the particles. The second one is due to a mechanic instability during the opening and subsequent closing of a contact caused by cyclic strain, which lets the particles alter their separation via spontaneous relative displacements ('jumps'), leading to energy dissipation into the surrounding polymer matrix[3]. Whereas the viscous contribution is strongly reduced when the temperature rises, the 'jump' dissipation is less affected. We have argued that this mechanism is a major, and perhaps the major, contributor to rolling resistance in automobile tires[3].

As before, in the case of γ, we may obtain a better feeling for W_{loss}, which also has the unit J/m^2, by inserting typical values for the other quantities in Eq. (2). Guided by the example in Fig. 2 we expect something on the order of 1 MPa or less for the network contribution to μ''. As before we set $(\phi/\phi_c)^{3.5} \approx 10$. In the limit of vanishing amplitude we have $\frac{1}{u^2}\int_0^u du' \int_0^\infty d\delta u \cdots \approx \frac{1}{4}\frac{D}{d}y$. From previous comparisons to experimental data (cf. table 1 in Ref.[2]), using D/d and y as fit parameters, we know that $\frac{D}{d}y \sim 10$ is probably typical. Using as before $R = 10$ nm, we conclude that $W_{loss}(T)$ should be about 1 mJ/m^2 or somewhat less. This is reasonable in the sense that the number is significantly smaller than the above value for γ. Whereas γ may be interpreted is a measure for the entire (free) energy of the contact, W_{loss} is a measure for the energy dissipated during a cycle, i.e. 'opening' the contact and subsequently 'closing' the contact cannot be expected to dissipate the entire energy of the contact, because only a small fraction of all bonds involved are temporarily broken.

Before we can compare our model to experimental data, we need to fix $\mu'_{\text{bulk poly}}$ and $\mu''_{\text{bulk poly}}$. For the sake of a mere demonstration of the model, we describe these moduli using the simple Zener model, i.e.

$$\mu'_{\text{bulk poly}}/\mu_1 = \frac{\tau^2\omega^2/\theta + 1}{\tau^2\omega^2 + 1} \qquad \text{and} \qquad \mu''_{\text{bulk poly}}/\mu_2 = \frac{\tau\omega}{\tau^2\omega^2 + 1} \tag{4}$$

where $\tau = \eta/\mu_2$ and $\theta = \mu_1/(\mu_1 + \mu_2)$. The quantity $\tau\omega$ is the product of a characteristic relaxation time τ and the excitation frequency ω. Using the principle of frequency-temperature superposition via $\ln\tau\omega = a/T - b$, where a and b as well as μ_1 and μ_2, are adjustable parameters, yields basically the experimental $\tan\delta$-peak.

3 Comparison to the experiment

Wang[11] describes a series of experimentally measured dynamic moduli, based largely on a standard system, which is systematically studied by altering a single material parameter keeping the others fixed. This study furnishes a nice testing ground for the above ideas. By fitting the model to the standard system, it is possible to compare the model prediction to the experimentally measured $\tan\delta$-curves when different parameters, e.g. filler volume fraction, particle size or filler type, are varied.

The left panel in Fig. 4 shows the standard system, SSBR Duradene 715 containing 50phr carbon black N234 in comparison to the unfilled polymer and other carbon black grades. For instance, the N660-primary particles are roughly twice the size of the N234-primary particles. On the basis of tables II and III in reference[8] we conclude that this remains true for their attendant aggregates. Thus, in this case the parameter R increases by a factor of 2 and the resulting theoretical $\tan\delta$ is shown by the dashed black line. We observe that the two theoretical curves almost coincide at low temperatures, i.e. in the temperature range
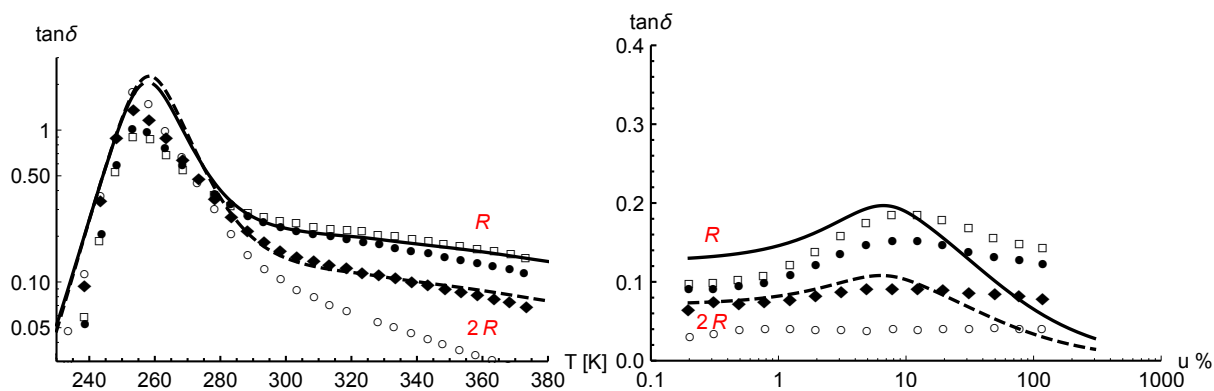
Figure 4. Left: Comparison of $\tan\delta$ vs. temperature for different particle sizes. The symbols are experimental data points for unfilled and filled (50phr) SSBR Duradene 715 extracted from Figure 23 in reference[11]. The dynamic strain amplitude is 5%. Hollow circles: gum; solid diamonds: N660; solid circles: N347; open squares: N234. Both lines are obtained using the model. The solid line is fitted to the N234-data (our reference system). Keeping all other parameters fixed the dashed line is obtained by doubling the particle radius. Right: Experimental $\tan\delta$ vs. strain amplitude extracted from Figure 21 in reference[11], obtained for unfilled and filled (50phr) SSBR Duradene 715, (symbols) compared to our model (lines). Hollow circles: gum; solid diamonds: N660; solid circles: N347; open squares: N234. The solid line (dashed line) is obtained using the same parameters as in the case of the solid line (dashed line) shown in the left panel.

of the peak. Because of the additivity assumption underlying the moduli and because we keep the parameters of the Zener model fixed (for the same polymer), this is not surprising. On the other hand, on the high temperature side of the peak our model provides the qualitatively correct result. The right panel in Fig. 4 shows the corresponding data and theoretical results for $\tan\delta$ versus strain amplitude. Note that no further adjustment is made. Again the model yields qualitative agreement with the data, even though the decrease of the data on the high amplitudes side of the peak is far less pronounced. Notice that the peak and in particular the decrease on the low amplitude side is governed by the strain distribution function (3), i.e. without $f(\delta u, u')$ the model would not exhibit this peak at all.

One final example is shown in Fig. 5. The open squares and the black line are for the above reference system (a slight adjustment of peak position was necessary due to a correspond ing shift in the experimental data). The red data are for the silica filled rubber. In both cases the filler content is 50 phr. In order to describe the silica, we modify two parameters in the theory. First the activation energy is increased from $E_a = -8$ kJ/mol, rather typical for the interaction of few methylene groups with carbon black, to $E_a = -25$ kJ/mol. This value corresponds to the energy of hydrogen bonds. The silica used here is a precipitated silica, usually possessing a large density of hydroxyl groups on its surface (around 5 to 6 per square nanometer). It is therefore reasonable that hydrogen bonding between particles is present. In addition, it was consistently found in computer simulations that when the bonds linking particles become stronger $W_{\text{loss}}(T)$ increases (e.g. reference [20]). We account for this by increasing $W_{\text{loss}}(T)$ to $1.5 \, W_{\text{loss}}(T)$. The factor 1.5 here is a convenient fit parameter, which yields the intersection with the solid black curve at about the temperature where the experimental curves cross. In principle however, a separate modelling calculation for this particular system is needed to obtain the correct $W_{\text{loss}}(T)$.

Additional comparisons to the data in Ref.[11] can be found in Ref.[4].

4 Conclusion

This paper summarizes recent work on the dynamic moduli of filled elastomers in general and the Payne effect in particular. The model discussed here is meant to explain or incorporate as many as possible of the basic observations when highly filled elastomers are studied with dynamic mechanical analysis. Examples include the Payne effect and its dependence on temperature, the maximum of the loss modulus or the changes of the dynamic moduli when the filler content, particle size or filler type is altered. The model also divides the overall description of the structure-property-relationship into manageable pieces. It identifies functional quantities like the load-bearing path distribution or the distribution of strain inhomogeneities and their respective mechanical effects. It also identifies quantities, most notably $W_{\text{loss}}(T)$, which are accessible via molecular simulation, allowing to study consequences of chemical changes, e.g. a different silane, on mechanical properties. Of course, alterations in the compounding will affect the distribution of filler and the overall structure of the filler network, i.e. the load-bearing path distribution or the distribution of strain inhomogeneities - in addition to parameters like the exponents Y and y or the
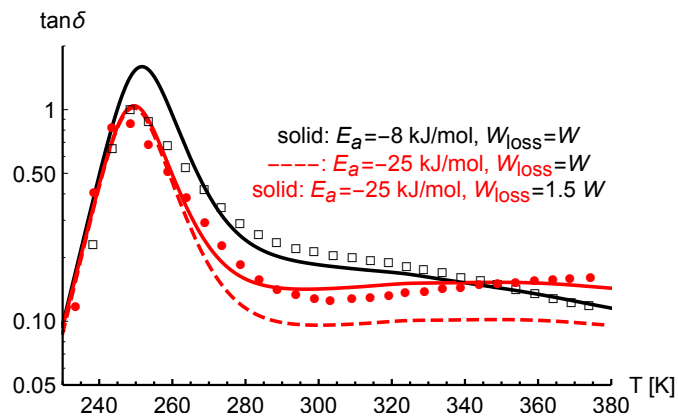
Figure 5. Experimental $\tan\delta$ vs. temperature extracted from Figure 29 in reference[11], obtained for filled (50phr) SSBR Duradene 715, (symbols) compared to the model (lines). The dynamic strain amplitude is 5%. Hollow squares: filler is Carbon black (N234); red solid circles: filler is silica (HiSil 210).

microscopic strain amplification factor D/d. Simulation techniques, which allow to connect chemical composition changes or even changes in material processing will have to resort to coarse-graining. Recent efforts along this line, in which the author is involved, are described in Ref.[12].

References

1. Gubbins, K. E. & Quirke, N. (eds.) *Molecular Simulation and Industrial Applications* (Gordon and Breach Science Publishers, Amsterdam, 1996).

2. Hentschke, R. The payne effect revisited. *Express Polym. Lett.* **11**, 278–292 (2017).

3. Meyer, J., Hentschke, R., Hager, J., Hojdis, N. W. & Karimi-Varzaneh, H. A. A nano-mechnical instability as primary contribution to rolling resistance. *Sci. Reports* **7**, 11275 (2017).

4. Hentschke, R. Macroscopic mechanical properties of elastomer nano-composites via molecular and analytical modelling. *Soft Mater.* **16**, 315–326 (2018). URL https://doi.org/10.1080/1539445X.2018.1518243. DOI 10.1080/1539445X.2018.1518243. https://doi.org/10.1080/1539445X.2018.1518243.

5. Zhang, P., Morris, M. & Doshi, D. Materials development for lowering rolling resistance of tires. *Rubber Chem. Technol.* **89**, 79–116 (2016). URL https://doi.org/10.5254/rct.16.83805. DOI 10.5254/rct.16.83805. https://doi.org/10.5254/rct.16.83805.

6. Vilgis, T. A., Heinrich, G. & Klüppel, M. *Reinforcement of Polymer Nano-Composites* (Cambridge University Press, New York, 2009).

7. Xi, H. & Hentschke, R. The influence of structure on mechanical properties of filler networks via coarse-grained modeling. *Macromol. Theory Simul.* **23**, 373–382 (2014).

8. Hess, W. M. & McDonald, G. C. Improved particle size measurements on pigments for rubber. *Rubber Chem. Technol.* **56**, 892–917 (1983). URL https://doi.org/10.5254/1.3538171. DOI 10.5254/1.3538171. https://doi.org/10.5254/1.3538171.

9. Carbon blacks for electrically conductive rubber products. Tech. Rep. TR812, Degussa AG.

10. Stöckelhuber, K. W., Svistkov, A. S., Pelevin, A. G. & Heinrich, G. Impact of filler surface modification on large scale mechanics of styrene butadiene/silica rubber composites. *Macromolecules* **44**, 4366–4381 (2011). URL https://doi.org/10.1021/ma1026077. DOI 10.1021/ma1026077. https://doi.org/10.1021/ma1026077.

11. Wang, M.-J. Effect of polymer-filler and filler-filler interactions on dynamic properties of filled vulcanizates. *Rubber Chem. Technol.* **71**, 520–589 (1998). URL https://doi.org/10.5254/1.3538492. DOI 10.5254/1.3538492. https://doi.org/10.5254/1.3538492.

12. Gundlach, N., Hentschke, R. & Karimi-Varzaneh, H. A. Filler flocculation in elastomer blends - an approach based on measured surface tensions and monte carlo simulation. *Soft Mater.* **0**, 1–14 (2019). URL https://doi.org/

10.1080/1539445X.2019.1568261. DOI 10.1080/1539445X.2019.1568261. https://doi.org/10.1080/1539445X.2019.1568261.